
A Novel Self-Distillation Architecture to Defeat Membership Inference Attacks

Xinyu Tang¹ Saeed Mahloujifar¹ Liwei Song¹ Virat Shejwalkar² Milad Nasr²
Amir Houmansadr² Prateek Mittal¹
¹Princeton University ² University of Massachusetts, Amherst
{xinyut,sfar,liweis,pmittal}@princeton.edu {vshejwalkar,milad,amir}@cs.umass.edu

Abstract

1 Membership inference attacks are a key measure to evaluate privacy leakage in
2 machine learning (ML) models, which aim to distinguish training members from
3 non-members by exploiting differential behavior of the models on member and non-
4 member inputs. We propose a new framework to train privacy-preserving models
5 that induces similar behavior on member and non-member inputs to mitigate
6 practical membership inference attacks. Our framework, called SELENA, has
7 two major components. The first component and the core of our defense, called
8 Split-AI, is a novel ensemble architecture for training. We prove that our Split-
9 AI architecture defends against a large family of membership inference attacks,
10 however, it is susceptible to new adaptive attacks. Therefore, we use a second
11 component in our framework called Self-Distillation to protect against such stronger
12 attacks, which (self-)distills the training dataset through our Split-AI ensemble and
13 has no reliance on external public datasets. We perform extensive experiments on
14 major benchmark datasets and the results show that our approach achieves a better
15 trade-off between membership privacy and utility compared to previous defenses.

16 1 Introduction

17 Recent work has shown that ML models are prone to memorizing sensitive information of training
18 data incurring serious privacy risks [23, 2, 3, 6, 20, 24, 7]. In this work, we focus on *membership*
19 *inference attack (MIA)*, which tries to identify whether a target sample was used to train the target ML
20 model or not based on model behavior[23]. MIAs pose a severe privacy threat by revealing private
21 information about training data. For example, knowing the victim’s presence in the hospital health
22 analytic training set reveals that the victim was once a patient in the hospital.

23 There are two main categories of membership inference defenses: *provable privacy* guaranteed
24 by DP and *empirical membership privacy defenses*. The first category uses differential privacy
25 mechanisms [1, 15, 28], which provide a *provable privacy guarantee* for all inputs. While provable
26 privacy with high utility is more desirable, it has been a challenge to use provable privacy techniques
27 guaranteed by DP like DP-SGD [1] to achieve high accuracy in many machine learning tasks. This
28 motivates the second category of membership inference defenses, where privacy is empirically
29 evaluated through practical MIAs to preserve high utility. However, none of the existing defenses in
30 this category [16, 10, 22] are able to provide sufficient MIA protection and high utility simultaneously
31 in the absence of public datasets [25, 5].

32 In this paper, we introduce a new defense, called SELENA,¹ to protect against black-box MIAs while
33 also offering a high utility, which falls in the category of *empirical membership privacy defenses*.

¹SELf ENsemble Architecture.

34 Our framework consists of two core components: *Split-AI*² and *Self-Distillation*. Our first component
 35 Split-AI trains multiple models (called sub-models) with random subsets from the training set, and
 36 applies adaptive inference to enable the model to have similar behavior on members and non-members:
 37 for any queried sample, no matter whether it is in training set, our defense only use sub-models
 38 which are not trained with it to get outputs; this ensures membership privacy for a large family of
 39 MIAs which we demonstrate through a formal analysis. Our second component Self-Distillation
 40 (self)-distills the exact same training sets by using the outputs from Split-AI as soft labels to train
 41 a new model, which solves the potential advanced attacks threat against Split-AI and computation
 42 overhead in inference.

43 2 Our defense

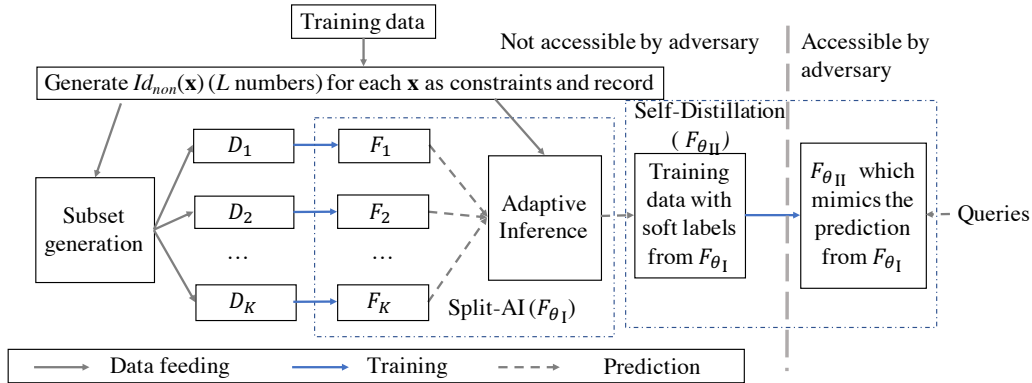


Figure 1: Our end-to-end defense framework with the Split-AI and Self-Distillation components.

44 Figure 1 gives an overview of our defense, where we denote Split-AI as F_{θ_I} and protected model
 45 from Self-Distillation as $F_{\theta_{II}}$.³ We next detail Split-AI and Self-Distillation separately.

46 **First component Split-AI.** MIAs aim to distinguish members and non-members of the private
 47 training data of a model. These attacks use the fact that the trained model has a different behavior,
 48 such as accuracy [21], confidence [29, 26, 25] and robustness [5, 13], on member and non-member
 49 data. MIAs leverage these differences to obtain an attack advantage that is better than a random guess
 50 even in the black-box setting. Our Split-AI design is based on the following intuition: *if a training*
 51 *sample is not used to train a sub-model, that sub-model will have similar behavior on that training*
 52 *sample and non-members.*

53 *Split-AI's training.* Specifically, for each data point \mathbf{x} in the training set, we randomly generate L
 54 non-model indices from $\{1, 2, \dots, K\}$ to denote the L non-models that are not trained with \mathbf{x} and
 55 record the identification numbers of these L non-model indices (denoted as $Id_{non}(\mathbf{x})$)⁴. We then
 56 generate the dataset partition based on these non-model indices. For each subset D_i , we will only use
 57 those training samples which do not include i in their non-model indices. We then train K sub-models
 58 F_i , one for each subset D_i , which have the same architecture and hyper-parameter settings.

59 *Split-AI's inference.* We now describe the adaptive inference based ensemble strategy for members
 60 and non-members. For each queried sample \mathbf{x} , the ensemble will check whether there is an exact
 61 match of \mathbf{x} in the training set:

- 62 • If so, which indicates that \mathbf{x} is a member, the defender will average the prediction vectors on
 63 \mathbf{x} from L models which are not trained with \mathbf{x} as the output, i.e., $\frac{1}{L} \sum_{i \in Id_{non}(\mathbf{x})} F_i(\mathbf{x})$;
- 64 • If not, the defender will randomly use non-member indices of a member sample \mathbf{x}'
 65 and average the prediction vectors on \mathbf{x} from L models of $Id_{non}(\mathbf{x}')$ as the output, i.e.,
 66 $\frac{1}{L} \sum_{i \in Id_{non}(\mathbf{x}')} F_i(\mathbf{x})$.

²Split Adaptive Inference Ensemble.

³PATE[17, 18] also trains multiple sub-models to provide privacy but with a public dataset, difference detailed in Appendix A.

⁴ $Id_{non}(\mathbf{x})$ records L sub-model indices which are not trained with \mathbf{x} .

67 We formally prove that Split-AI strategy can reduce the accuracy of *direct* single-query MIAs (typical
68 been used in most previous MI defenses [16, 10, 25], see Appendix B.1 for more details) to a random
69 guess (See Theorem 2 in Appendix C). The intuitive explanation for this proof is that for each data
70 point, the distribution of output of this algorithm on this given point \mathbf{x} is independent of the presence
71 of \mathbf{x} in the training set. This is because, we will not use models that are trained with \mathbf{x} to answer
72 queries, even if \mathbf{x} is in the training set.

73 *Limitations of Split-AI.* While our Split-AI strategy is resilient to direct single-query MIAs, an
74 adversary can leverage more advanced attacks including indirect attacks [14] and replay attacks. For
75 indirect attacks, attacker can make a single *indirect* query by adding a small noise to the target sample.
76 Split-AI will recognize noisy training samples as non-members and may end up using sub-models
77 trained with the target sample, thus leaking membership information. For replay attacks: Split-AI has
78 one possible output for member sample, while there are multiple possible outputs for non-members.
79 Furthermore, Split-AI imposes a computational overhead in the inference phase as Split-AI needs to
80 perform inference on L models for each queried sample.

81 **Second component: Self-Distillation.** To overcome these limitations, we leverage distillation [9].
82 To be more specific, here we term our second component as *Self-Distillation* because we use features
83 in the exact same training set as Split-AI along with the prediction vectors from Split-AI as soft labels
84 to train a new model using conventional training. The new protected model benefits from distillation
85 to largely preserve Split-AI’s defense ability against direct single-query attack (See Theorem 5 and
86 Corollary 6 in Appendix C) while maintaining a good classification accuracy. For queried samples,
87 the defender now just need to do the inference on the new protected model $F_{\theta_{II}}$ distilled from the
88 Split-AI.

89 *Self-Distillation overcomes the privacy limitations of Split-AI and mitigates advanced MIAs.* The
90 defender controls the Self-Distillation component and ensures that Self-Distillation only queries
91 each exact training sample once. The attacker only has black-box access to the protected output
92 model of Self-Distillation, but cannot access the Split-AI model. Hence, the attacker cannot exploit
93 the soft labels computation of Split-AI as discussed before. Hence, the final protected model from
94 Self-Distillation effectively mitigates the replay and multi-query indirect attacks. Self-Distillation
95 also solves the computational overhead limitation of the Split-AI at inference time: the defender now
96 only needs to make inference on a single Self-Distilled model.

97 3 Evaluations

98 **Experimental setup.** We follow the setting in previous work [16] that the attacker knows half
99 members and non-members, i.e., the number of members and non-members used to train and evaluate
100 the attack model are the same and the random guess baseline attack accuracy is 50%. We use
101 three benchmark datasets and target models which are widely used in prior works on MI attacks and
102 defenses [23, 16, 10]: Purchase100 [19], Texas100 [27] and CIFAR100 [12]. We use $K = 25$, $L = 10$
103 for all three datasets. Additional experimental details are in Appendix D. We systematically evaluate
104 our end-to-end defense framework by direct single-query attacks, indirect label-only attacks (see
105 Appendix B.1 for more details), and adaptive attacks (explained in next paragraph) and make a
106 comparison with previous MI defenses: MemGuard [10] and adversarial regularization [16].

107 **Adaptive attacks.** The systematic evaluation of existing defenses by Song et al. [25] emphasizes that
108 the defender should consider adaptive attackers with knowledge of the defense to rigorously evaluate
109 the performance of the defenses. Here we consider the attacker to construct a shadow Split-AI using
110 the known training samples to provide additional information (More details in Appendix B.2).

111 **Results.** Table 1 summarizes the classification accuracy and best attack accuracy for each attack type,
112 including comparison with previous defenses [16, 10]. We also includes undefended models as a
113 baseline. We use $\text{acc}_{\text{train}}$ and acc_{test} to denote the model classification accuracy on training set and
114 test set. We use acc_{dsq} , acc_{lo} , acc_{ada} , and acc_{best} to denote accuracy for direct single-query attacks,
115 label-only attacks, adaptive attacks and best attack accuracy among all attacks respectively.

116 *Comparison with MemGuard.* While the test accuracy of our defense is a little lower (at most 3.9%)
117 than MemGuard (MemGuard has the same test accuracy as the undefended model), the MIA accuracy
118 against MemGuard is much higher than our defense. Compared to a random guess, which achieves
119 50% attack accuracy, the best attacks on MemGuard can achieve 14.7% \sim 19.9% advantage over a

Table 1: Comparison of membership privacy and accuracy on training/test set of undefended model, previous defenses and SELENA on three different datasets. AdvReg refers to adversarial regularization. The last column is the highest attack accuracy for each row, i.e. for a specific defense on one dataset, the highest attack accuracy that MIAs can achieve. The last column gives an overview of comparison: the lower the best attack accuracy, lower the membership inference threat. For each dataset, the defense which has the lowest corresponding attack accuracy is bold in the column of best direct single-query attack, best label-only and best attack.

dataset	defense	acc _{train}	acc _{test}	acc _{dsq}	acc _{lo}	acc _{ada}	acc _{best}
Purchase100	None	99.98%	83.2%	67.3%	65.8%	N/A	67.3%
	MemGuard	99.98%	83.2%	58.7%	65.8%	N/A	65.8%
	AdvReg	91.9%	78.5%	57.3%	57.4%	N/A	57.4%
	SELENA	82.7%	79.3%	53.3%	53.2%	54.3%	54.3%
Texas100	None	79.3%	52.3%	66.0%	64.7%	N/A	66.0%
	MemGuard	79.3%	52.3%	63.0%	64.7%	N/A	64.7%
	AdvReg	55.8%	45.6%	60.5%	56.6%	N/A	60.5%
	SELENA	58.8%	52.6%	54.8%	55.1%	54.9%	55.1%
CIFAR100	None	99.98%	77.0%	74.8%	69.9%	N/A	74.8%
	MemGuard	99.98%	77.0%	68.7%	69.9%	N/A	69.9%
	AdvReg	86.9%	71.5%	58.6%	59.0%	N/A	59.0%
	SELENA	78.1%	74.6%	55.1%	54.0%	58.3%	58.3%

120 random guess, which is a factor of 2.4 ~ 3.7 higher than our defense. In general, MemGuard does
 121 not have any defense against MIAs that do not rely on confidence information: attacker can use
 122 label-only attacks as adaptive attacks since MemGuard only obfuscates confidence.

123 *Comparison with adversarial regularization.* Our defense achieves higher classification accuracy
 124 and lower MIA accuracy compared with adversarial regularization. The classification accuracy of
 125 our defense is higher than adversarial regularization across all three datasets, and as high as 7.0%
 126 for the Texas100 dataset. For MIAs, our defenses achieves significantly lower attack accuracy than
 127 adversarial regularization. MIA attacks against adversarial regularization is higher than our defense
 128 across all three datasets, and its advantage over random guess is at most a factor of 2.1 than our
 129 defense (on Texas100). Besides, adversarial regularization is much harder to tune.

130 We also include a comparison of our defense with early stopping [25] and DP-SGD [1] in Appendix E.
 131 In addition, we also highlight the following two points from Table 1:

132 *Our SELENA effectively induces similar behaviors including generalization, confidence, robustness*
 133 *for member and non-member samples and therefore the MIA attack accuracy is largely reduced.* Let us
 134 take the generalization gap g as an example: the generalization gap in undefended models/MemGuard
 135 is 16.78% on Purchase100, 27.0% on Texas100, 22.98% on CIFAR100; the generalization gap in
 136 adversarial regularization is 13.4% on Purchase100, 10.2% on Texas100 and 15.4% on CIFAR100. In
 137 contrast, the generalization gap in our defense is 3.4% on Purchase100, 6.2% on Texas100 and 3.5%
 138 on CIFAR100: Our mechanism reduces the total generalization gap by a factor of up to 6.6 compared
 139 to undefended models/MemGuard, and a factor of up to 4.4 compared to adversarial regularization.

140 *The additional estimation of soft labels provided by shadow Split-AI (using the entirety of the*
 141 *attacker’s knowledge) provides additional information to the attacker, which enhances the accuracy*
 142 *of our adaptive attacks: attack has more advantage over random guess than direct single-query attack*
 143 *and label-only attacks. However, even considering the strong adaptive attacks, SELENA still achieves*
 144 *lower attack accuracy in comparison to previous defenses.*

145 **Computation overhead in SELENA.** One cost that our framework needs to pay is the use of
 146 additional computing resources in the training process as we train multiple sub-models for Split-AI
 147 in the training phase. However, our SELENA does not incur additional computation overhead in
 148 inference compared to undefended model. Here we argue that the cost of computing resources in
 149 the training phase is acceptable as the improvement in GPU technology are making the computing
 150 resources cheap while the privacy threat remains severe. We note that if multiple GPUs are available,
 151 our approach can easily benefit from parallelization by training the K sub-models in parallel.

References

- 152
- 153 [1] Martin Abadi, Andy Chu, Ian Goodfellow, H Brendan McMahan, Ilya Mironov, Kunal Talwar, and
154 Li Zhang. Deep learning with differential privacy. In *Proceedings of the 2016 ACM SIGSAC Conference*
155 *on Computer and Communications Security*, pages 308–318, 2016.
- 156 [2] Nicholas Carlini, Chang Liu, Úlfar Erlingsson, Jernej Kos, and Dawn Song. The secret sharer: Evaluating
157 and testing unintended memorization in neural networks. In *USENIX Security Symposium*, pages 267–284,
158 2019.
- 159 [3] Nicholas Carlini, Florian Tramer, Eric Wallace, Matthew Jagielski, Ariel Herbert-Voss, Katherine Lee,
160 Adam Roberts, Tom Brown, Dawn Song, Ulfar Erlingsson, et al. Extracting training data from large
161 language models. In *USENIX Security Symposium*, 2021.
- 162 [4] Rich Caruana, Steve Lawrence, and C Lee Giles. Overfitting in neural nets: Backpropagation, conjugate
163 gradient, and early stopping. In *Advances in Neural Information Processing Systems*, pages 402–408,
164 2001.
- 165 [5] Christopher A Choquette Choo, Florian Tramer, Nicholas Carlini, and Nicolas Papernot. Label-only
166 membership inference attacks. In *Proceedings of the 38th International Conference on Machine Learning*,
167 2021.
- 168 [6] Matt Fredrikson, Somesh Jha, and Thomas Ristenpart. Model inversion attacks that exploit confidence
169 information and basic countermeasures. In *Proceedings of the 22nd ACM SIGSAC Conference on Computer*
170 *and Communications Security*, pages 1322–1333, 2015.
- 171 [7] Karan Ganju, Qi Wang, Wei Yang, Carl A Gunter, and Nikita Borisov. Property inference attacks on fully
172 connected neural networks using permutation invariant representations. In *Proceedings of the 2018 ACM*
173 *SIGSAC Conference on Computer and Communications Security*, pages 619–633, 2018.
- 174 [8] Kaiming He, Xiangyu Zhang, Shaoqing Ren, and Jian Sun. Deep residual learning for image recognition.
175 In *Proceedings of the IEEE Conference on Computer Vision and Pattern Recognition*, pages 770–778,
176 2016.
- 177 [9] Geoffrey Hinton, Oriol Vinyals, and Jeff Dean. Distilling the knowledge in a neural network. *arXiv preprint*
178 *arXiv:1503.02531*, 2015.
- 179 [10] Jinyuan Jia, Ahmed Salem, Michael Backes, Yang Zhang, and Neil Zhenqiang Gong. Memguard:
180 Defending against black-box membership inference attacks via adversarial examples. In *Proceedings of*
181 *the 2019 ACM SIGSAC Conference on Computer and Communications Security*, pages 259–274, 2019.
- 182 [11] Diederik P Kingma and Jimmy Ba. Adam: A method for stochastic optimization. *arXiv preprint*
183 *arXiv:1412.6980*, 2014.
- 184 [12] Alex Krizhevsky and Geoffrey Hinton. Learning multiple layers of features from tiny images. Technical
185 report, University of Toronto, 2009.
- 186 [13] Zheng Li and Yang Zhang. Membership leakage in label-only exposures. In *Proceedings of the 2021 ACM*
187 *SIGSAC Conference on Computer and Communications Security*, 2021.
- 188 [14] Yunhui Long, Vincent Bindschaedler, Lei Wang, Diyue Bu, Xiaofeng Wang, Haixu Tang, Carl A Gunter,
189 and Kai Chen. Understanding membership inferences on well-generalized learning models. *arXiv preprint*
190 *arXiv:1802.04889*, 2018.
- 191 [15] H Brendan McMahan, Daniel Ramage, Kunal Talwar, and Li Zhang. Learning differentially private
192 recurrent language models. In *International Conference on Learning Representations*, 2018.
- 193 [16] Milad Nasr, Reza Shokri, and Amir Houmansadr. Machine learning with membership privacy using
194 adversarial regularization. In *Proceedings of the 2018 ACM SIGSAC Conference on Computer and*
195 *Communications Security*, pages 634–646, 2018.
- 196 [17] Nicolas Papernot, Martín Abadi, Ulfar Erlingsson, Ian Goodfellow, and Kunal Talwar. Semi-supervised
197 knowledge transfer for deep learning from private training data. In *International Conference on Learning*
198 *Representations*, 2017.
- 199 [18] Nicolas Papernot, Shuang Song, Ilya Mironov, Ananth Raghunathan, Kunal Talwar, and Úlfar Erlingsson.
200 Scalable private learning with pate. In *International Conference on Learning Representations*, 2018.
- 201 [19] Purchase. Acquire valued shoppers challenge. [https://www.kaggle.com/c/](https://www.kaggle.com/c/acquire-valued-shoppers-challenge/data)
202 [acquire-valued-shoppers-challenge/data](https://www.kaggle.com/c/acquire-valued-shoppers-challenge/data). [Online; accessed 22-March-2020].

- 203 [20] Ahmed Salem, Apratim Bhattacharya, Michael Backes, Mario Fritz, and Yang Zhang. Updates-leak:
204 Data set inference and reconstruction attacks in online learning. In *USENIX Security Symposium*, pages
205 1291–1308, 2020.
- 206 [21] Ahmed Salem, Yang Zhang, Mathias Humbert, Pascal Berrang, Mario Fritz, and Michael Backes. MI-leaks:
207 Model and data independent membership inference attacks and defenses on machine learning models. In
208 *Network and Distributed Systems Security Symposium (NDSS)*, 2019.
- 209 [22] Virat Shejwalkar and Amir Houmansadr. Membership privacy for machine learning models through
210 knowledge transfer. In *Proceedings of the AAAI Conference on Artificial Intelligence (AAAI)*, 2021.
- 211 [23] Reza Shokri, Marco Stronati, Congzheng Song, and Vitaly Shmatikov. Membership inference attacks
212 against machine learning models. In *2017 IEEE Symposium on Security and Privacy (SP)*, pages 3–18.
213 IEEE, 2017.
- 214 [24] Congzheng Song, Thomas Ristenpart, and Vitaly Shmatikov. Machine learning models that remember too
215 much. In *Proceedings of the 2017 ACM SIGSAC Conference on Computer and Communications Security*,
216 pages 587–601, 2017.
- 217 [25] Liwei Song and Prateek Mittal. Systematic evaluation of privacy risks of machine learning models. In
218 *USENIX Security Symposium*, 2021.
- 219 [26] Liwei Song, Reza Shokri, and Prateek Mittal. Privacy risks of securing machine learning models against
220 adversarial examples. In *Proceedings of the 2019 ACM SIGSAC Conference on Computer and Communi-
221 cations Security*, pages 241–257, 2019.
- 222 [27] Texas. Texas hospital stays dataset. [https://www.dshs.texas.gov/THCIC/Hospitals/Download.
223 shtm](https://www.dshs.texas.gov/THCIC/Hospitals/Download.shtm). [Online; accessed 22-March-2020].
- 224 [28] Yu-Xiang Wang, Borja Balle, and Shiva Prasad Kasiviswanathan. Subsampled rényi differential privacy
225 and analytical moments accountant. In *The 22nd International Conference on Artificial Intelligence and
226 Statistics*, pages 1226–1235. PMLR, 2019.
- 227 [29] Samuel Yeom, Irene Giacomelli, Matt Fredrikson, and Somesh Jha. Privacy risk in machine learning:
228 Analyzing the connection to overfitting. In *2018 IEEE 31st Computer Security Foundations Symposium
229 (CSF)*, pages 268–282. IEEE, 2018.
- 230 [30] Samuel Yeom, Irene Giacomelli, Alan Menaged, Matt Fredrikson, and Somesh Jha. Overfitting, robustness,
231 and malicious algorithms: A study of potential causes of privacy risk in machine learning. *Journal of
232 Computer Security*, 28(1):35–70, 2020.

233 Appendix

234 A Comparison With PATE

235 PATE [17, 18] is a framework composed of teacher-student distillation and leverages public data to achieve a
236 better privacy-utility trade-off for differential privacy. PATE uses a disjoint training set partition for sub-models
237 in the teacher component. To get the private label of the public dataset to train the student model, PATE applies
238 noisy count among sub-models.

239 There are three major differences between our work and PATE: (1). PATE requires a *public dataset* to provide
240 the provable end-to-end privacy guarantee, which is not possible in certain practical scenarios such as healthcare.
241 Our defense does not need public datasets and provides a strong empirical defense against MIAs. (2). We apply
242 a novel *adaptive inference strategy* to defend against MIAs: for each training sample, we only use prediction of
243 sub-models in Split-AI that are not trained with it as these sub-models will not leak membership information
244 for it. PATE does not use adaptive inference and relies on majority voting over all sub-models. (3). We use
245 *overlapping* subsets to train sub-models. This allows our approach to obtain high accuracy for each sub-model
246 with sufficient subset size. PATE faces the limitation of each sub-model being trained with much reduced subset
247 size due to disjoint subsets.

248 In addition, PATE incurs a 0.7% ~ 6.7% drop in test accuracy [18], while the test accuracy drop in our defense
249 is no more than 3.9%.

250 B Membership inference attacks

251 MIAs can utilize the prediction vector as a feature using a neural-network-based model, called *NN-based attacks*,
252 or can compute a range of custom metrics (such as correctness, confidence, entropy) over the prediction vector
253 to infer membership, called *metric-based attacks*. These attacks can be mounted either by knowing a subset
254 of the training set [16] or by knowing a dataset from the same distribution of the training set and constructing
255 shadow models [23].

256 Let us denote D_{tr} as the training set for the target model, i.e., members and D_{te} as the test set, i.e., non-members.
257 D_{tr}^A and D_{te}^A are, respectively, the sets of members and non-members that the attacker knows. $I(\mathbf{x}, y, F(\mathbf{x}))$ is
258 the binary membership inference classifier which codes members as 1, and non-members as 0. The literature
259 typically measures MIA efficacy as the attack accuracy:

$$\frac{\sum_{(\mathbf{x}, y) \in D_{tr} \setminus D_{tr}^A} I(\mathbf{x}, y, F(\mathbf{x})) + \sum_{(\mathbf{x}, y) \in D_{te} \setminus D_{te}^A} (1 - I(\mathbf{x}, y, F(\mathbf{x})))}{|D_{tr} \setminus D_{tr}^A| + |D_{te} \setminus D_{te}^A|}$$

260 In most previous attacks [23, 16, 30, 25], the number of members and non-members used to train and evaluate
261 the attack model are the same. With this approach, the prior probability of a sample being either a member or a
262 non-member is 50% (corresponding to a random guess).

263 Next, we summarize existing black-box MIAs in the following two categories: **direct** attacks and **indirect**
264 attacks, as well as explain adaptive attacks against our SELENA defense.

265 B.1 Existing membership inference attacks

266 **Direct single-query attacks:** Most existing MIAs directly query the target sample and utilize the resulting
267 prediction vector. Since ML models typically have only one output for each queried sample, just a single
268 query is sufficient. This category of MIAs includes NN-based attack [23, 16], correctness-based attack [30],
269 confidence-based attack [29, 26, 25], entropy-based attack [23, 25], modified entropy-based attack [25]. We
270 consider all these attacks across three datasets and report the best direct single-query attack accuracy in Table 1.

271 **Indirect multi-query attacks (label-only attacks):** Long et al. [14] stated that indirect attacks can make
272 queries that are related to target sample \mathbf{x} to extract additional membership information as a training sample
273 influences the model prediction both on itself and other samples in its neighborhood. These indirect attacks
274 usually make multiple queries for a single target sample [14, 13, 5]. For example, multi-query *label-only attacks*
275 leverage the predicted label of the queried data as features, and are thus immune to defenses that only obfuscate
276 prediction confidences, e.g., MemGuard [10]. The key idea in label-only attacks is that the model should be
277 more likely to correctly classify the samples around the training data than the samples around test data, i.e.,
278 members are more likely to exhibit high robustness than non-members [13, 5]. Simply obfuscating a model’s
279 confidence scores can not hide label information to defend against such label-only attacks. This category of
280 MIAs includes boundary estimation attacks [13, 5] and data augmentation attacks [5]. We consider boundary
281 estimation attacks for all three datasets and data augmentation attacks on CIFAR100 as only CIFAR100 uses
282 data augmentation during the training process.

283 B.2 Adaptive attacks

284 The systematic evaluation of existing defenses by Song et al. [25] emphasizes the importance of placing the
285 attacker in the last step of the arms race between attacks and defenses: the defender should consider adaptive
286 attackers with knowledge of the defense to rigorously evaluate the performance of the defenses. Therefore,
287 here we consider attacks that are tailored to our defense. As our defense leverages soft labels from the Split-AI
288 ensemble to train a new model $F_{\theta_{II}}$ in Self-Distillation, we need to analyze whether and how an attacker can
289 also leverage the information about soft labels.

290 We first note that an attacker is unable to directly interact with our Split-AI ensemble to directly estimate soft
291 labels, since the prediction API executes queries on the model produced by the Self-Distillation component.
292 Second, we expect that when the model provider finishes training the protected model $F_{\theta_{II}}$ with soft labels
293 obtained from Split-AI ensemble, it can safely delete the sub-models and soft labels of the training set to avoid
294 inadvertently leaking information about the soft labels.

295 However, an attacker can still aim to indirectly *estimate* soft labels. As we assume that the attacker knows
296 partial membership of the exact training set in evaluating membership privacy risks (specifically, half of the
297 whole training set) and attacker cannot have access to the defender’s non-member model indices $Id_{non}(\mathbf{x})$ for
298 training set, the attacker will generate new non-member model indices $Id_{non}(\mathbf{x})'$ for these known member
299 samples to train a new shadow Split-AI ensemble and use the shadow Split-AI to estimate soft labels of the
300 target samples. The attacker can then use such soft labels as an additional feature to learn the difference in target
301 model’s behavior on members and non-members, and launch MIAs on $F_{\theta_{II}}$. The shadow Split-AI discussed in

302 our paper is stronger than original shadow models [23] since it is trained with exact knowledge of the partial
303 training dataset.

304 We design four adaptive attacks including two NN-based attacks and two metric-based attacks to leverage the
305 estimated soft labels to attack our defense. To clarify, $F_{\theta_{11}}$ denotes the protected target model which answers the
306 attacker’s queries and F'_{θ_1} denotes the shadow Split-AI ensemble constructed by attacker.

307 **MIAs based on NN and soft labels:** The first NN-based attack concatenates the soft labels obtained from F'_{θ_1} ,
308 the predicted confidence from $F_{\theta_{11}}$ and the one-hot encoded class labels as features to train a neural network
309 attack model (denoted as I_{NN1}). The second attack utilizes the difference between the estimated soft labels
310 from F'_{θ_1} and outputs from $F_{\theta_{11}}$, and uses this difference as an input to the NN architecture used by Nasr et
311 al. [16] (denoted as I_{NN2}).

312 **MIAs based on distance between soft labels and predicted confidence:** Similar to previous metric-based
313 attacks [25], an attacker may try to distinguish between members and non-members by leveraging the distance
314 between estimated soft labels from F'_{θ_1} , and the prediction confidence vectors from $F_{\theta_{11}}$. We have:

$$I_{\text{dist}}(F_{\theta_{11}}(\mathbf{x}), F'_{\theta_1}(\mathbf{x}), y) = \mathbb{1}\{\text{Dist}(F_{\theta_{11}}(\mathbf{x}), F'_{\theta_1}(\mathbf{x})) \leq \tau_{(y)}\}$$

$$\text{or, } I_{\text{dist}}(F_{\theta_{11}}(\mathbf{x}), F'_{\theta_1}(\mathbf{x}), y) = \mathbb{1}\{\text{Dist}(F_{\theta_{11}}(\mathbf{x}), F'_{\theta_1}(\mathbf{x})) \geq \tau_{(y)}\}$$

315 where we apply both class-dependent threshold τ_y and class-independent threshold τ and we will report the
316 highest MIA accuracy. In this work we consider L_2 distance $I_{L_2\text{-dist}}$ and cross-entropy loss $I_{\text{CE-dist}}$ (since the
317 cross-entropy loss function is used for training our defense models).

318 C Proof for Split-AI against Direct, Single-Query Membership Inference 319 Attack

320 **Notation.** In this section, we use $x \leftarrow X$ to denote that x is sampled from a distribution X . We use $\text{Supp}(X)$
321 to denote the support set of a random variable X . By $TV(X, X')$ we denote the total variation distance between
322 X and X' , that is $TV(X, X') = \sup_{S \subset \text{Supp}(X) \cup \text{Supp}(X')} \Pr[X \in S] - \Pr[X' \in S]$. We present our Split-AI
323 algorithm in Algorithm 1.

324 **Definition 1** (Direct, Single-Query Membership Inference). *The single-query membership inference game is*
325 *defined between an attacker A and a learner C and is parameterized by a number n which is the number of*
326 *training examples.*

- 327 1. The attacker selects a dataset $X = \{x_1, \dots, x_{2n}\}$ and sends it to the learner.
- 328 2. Learner selects a uniformly random Boolean vector $b = b_1, \dots, b_{2n}$ such that the Hamming weight of
329 b is exactly n .
- 330 3. Learner constructs a dataset $S = \{x_i; \forall i \in [2n], b_i = 1\}$ and learns a model F_{θ_1} using S as training
331 set.
- 332 4. Learner selects a random $i \in [2n]$ and sends $(x_i, F_{\theta_1}(x_i))$ to the adversary
- 333 5. Adversary outputs a bit b'_i .

334 The advantage of A in breaking the security game above is $\text{SQMI}(A, C, n) = \mathbf{E}[1 - |b_i - b'_i|]$ where the
335 expectation is taken over the randomness of the adversary and learner.

336 **Remark 1.** We can define a variant of the security game of Definition 1 for a fixed dataset X . That is, instead of
337 X being chosen by adversary, we define the game for a given X . We use $\text{SQMI}(A, C, X)$ to denote the success
338 of adversary in the security game with the dataset fixed to X .

339 **Theorem 2.** Consider a learner C_{ST} that uses Algorithm 1. For any direct, single-query membership inference
340 adversary A we have

$$\text{SQMI}(A, C_{ST}, n) = 50\%$$

341 *Proof.* We show that for any adversary’s choice of $i \in [2n]$ in step 4 of the security game, the view of adversary
342 in two cases when $b_i = 0$ and when $b_i = 1$ are statistically identical. Note that the only information that the
343 adversary receives is $r_i = F_{\theta_1}(x_i)$. We show that the distribution of two random variables $r_i | b_i = 0$ and
344 $r_i | b_i = 1$ are identical. Let U_i be a random variable corresponding to the subset of trained models that do not
345 contain x_i in their training set (in particular $|U_i| = L$ if $b_i = 1$ and $|U_i| = K$ when $b_i = 0$). Also, let U denote
346 a random variable corresponding to a subset of L models that do not contain a random x_k in their training data
347 where k is selected from $\{j \in [2n]; b_j = 1\}$ uniformly at random.

Algorithm 1 Split-AI Model F_{θ_t}

Initialize:

K : total number of sub-models F_1, F_2, \dots, F_K

L : for each training sample, the number of sub-models which are not trained with it.

(X_{train}, Y_{train}) : training data and labels

Training Phase:

Randomly generate the L identification numbers of sub-models for each training sample $Id_{non}(\mathbf{x})$.

for $i = 1$ to K **do**

Construct subset $(X_{train}^i, Y_{train}^i)$ for model F_i based on the recorded Id_{non} s for models:
 $\{(\mathbf{x}, y) : (\mathbf{x}, y) \in (X_{train}, Y_{train}), i \text{ not in } Id_{non}(\mathbf{x})\}$

for number of the training epochs **do**

Update F_i by descending its stochastic gradients over $l(F_i(X_{train}^i), Y_{train}^i)$.

end for

end for

Inference Phase: $F_{\theta_t}(\mathbf{x})$

Given \mathbf{x}

if \mathbf{x} in X_{train} **then**

$$F_{\theta_t}(\mathbf{x}) = \frac{1}{L} \sum_{i \in Id_{non}(\mathbf{x})} F_i(\mathbf{x})$$

else

Randomly select \mathbf{x}' in the training set,

$$F_{\theta_t}(\mathbf{x}) = \frac{1}{L} \sum_{i \in Id_{non}(\mathbf{x}')} F_i(\mathbf{x})$$

end if

348 We first note that $U \mid b_i = 0$ and $U_i \mid b_i = 1$ are identically distributed random variables. Specif-
349 ically, they are both an ensemble of L models trained on a uniformly random subset of a dataset $T \subset$
350 $\{x_1, \dots, x_{i-1}, x_{i+1}, \dots, x_{2n}\}$ where $|T| = n - 1$.

351 Now, lets calculate the distribution of response when $b_i = 1$ and when $b_i = 0$. For $b_i = 1$ we have

$$(r_i \mid b_i = 1) \equiv \left(\frac{1}{L} \cdot \sum_{F \in U_i} F(x_i) \mid b_i = 1 \right)$$

352 For $b_i = 0$ we have

$$(r_i \mid b_i = 0) \equiv \left(\frac{1}{L} \cdot \sum_{F \in U} F(x_i) \mid b_i = 0 \right)$$

353 Now since $U_i \mid b_i = 1$ and $U \mid b_i = 0$ are distributed identically, the summation of the query points are also
354 identically distributed. Therefore, $r_i \mid b_i = 0$ and $r_i \mid b_i = 1$ are identically distributed. Note that it is crucial
355 that the adversary only queries the point x_i as otherwise we had to take the summation over $U \mid b_i = 1$ and
356 $U \mid b_i = 0$ which are not identically distributed (the case of $b_i = 1$ could have x_i in the training set of the L
357 models).

358 Since we prove that $r_i \mid b_i = 1$ and $r_i \mid b_i = 0$ are identical, the adversary cannot distinguish them and the
359 success probability of the adversary is exactly 0.5. The intuitive explanation for this proof is that for each data
360 point, the distribution of output of this algorithm on a given point x is independent of the presence of x in the
361 training set, as we will not use models that are trained with x to answer queries, even if x is in the training set.

362 □

363 **Remark 3** (A stronger security game and theorem). *Note that there is a worst-case variant of Definition 1*
364 *where in step 4, instead of the challenger, the adversary select $i \in [2n]$. This is a stronger security game as the*
365 *adversary can select the worst example in the dataset. However, Theorem 2 remain unchanged in this game.*
366 *This is because the proof applies to any $i \in [2n]$ and does not require i to be chosen at random. As we will see*
367 *below, we have another theorem (Theorem 5) that considers the privacy of end-to-end SELENA for which the*
368 *guarantee only holds for the weaker definition.*

369 **Definition 2** (stable distillation). A distillation algorithm $Q: M_s \times \text{AUX} \rightarrow M_o$ is a potentially randomized
 370 algorithm with access to a source model $m_s \in M_s \subseteq Y^X$ and some auxiliary information and returns an
 371 output model $m_o \in M_o \subset Y^X$. We define the notion of stability for a distillation algorithm on a point $x \in X$,
 372 and joint distribution \mathcal{M} on $M_s \times \text{AUX}$ as follows:

$$\text{stability}(Q, \mathcal{M}, x) = 1 - TV(Q(\mathcal{M})[x], \mathcal{M}[x]).$$

Moreover, we say the algorithm Q has (α, β) -stability on a distribution \mathcal{M} and a dataset X iff

$$\Pr_{x \leftarrow X} [\text{stability}(Q, \mathcal{M}, x) \leq 1 - \alpha] \leq \beta$$

373

374 **Example.** If the distillation algorithm Q ensures that for a specific point x and for all $m_s \in M_s$ we have
 375 $Q(m_s)[x] = m_s[x]$, then Q has stability 1 on point x for all distributions \mathcal{M} defined on M_s .

376 **Remark 4.** The distillation algorithm Q could also depend on an additional dataset that is correlated with m_s
 377 as the auxiliary information. For instance, in our self-distillation algorithm, the distillation is done through
 378 the same training set that was used to train m_s . In this case, we are interested in the joint distribution \mathcal{M} that
 379 consist of a model m_s as first element and a dataset D as the second element, so that m_s is a model trained on
 380 dataset D .

381 Now we state a corollary of our Theorem 2 about the privacy of the distilled models from the output of the
 382 Split-AI operation.

383 **Notation.** For a learner C and a dataset X , we use $\mathcal{M}_{C,X}$ to denote a distribution of models that is obtained
 384 from the following process: First select a random subset S of size $|X|/2$ and then train a model m on that subset
 385 using learner C and output (m, S) . For a learner C and a distillation model Q , we use QoC to denote a learner
 386 that first uses C to train a model and then uses distillation algorithm Q to distill that model and then returns the
 387 distilled model.

388 **Theorem 5.** Let C be an arbitrary learner. Assume for a set of samples X the distillation algorithm Q has
 389 (α, β) -stability on distribution $\mathcal{M}_{C,X}$ and dataset X . Then, for any adversary A we have

$$\text{SQMI}(A, QoC, X) \leq \text{SQMI}(A, C, X) + \alpha + \beta.$$

390 *Proof.* Consider an adversary A that given a response $QoC[x_i]$ on query $x_i \in X$ outputs a bit $b'_i =$
 391 $A(QoC(x_i))$. Let E be an event defined on X such that $E(x) = 1$ iff

$$\text{stability}(Q, \mathcal{M}_{C,X}, x) \geq 1 - \alpha.$$

392 For a point x_i such that $E(x_i) = 1$ we have

$$\begin{aligned} \Pr [A(QoC[x_i]) = b_i] &\leq \Pr [QoC[x_i] \neq C[x_i]] \\ &\quad + \Pr [A(C[x_i]) = b_i \mid C(x_i) = QoC[x_i]] \cdot \Pr [QoC[x_i] = C[x_i]] \\ &\leq \alpha + \Pr [A(C[x_i]) = b_i] \end{aligned}$$

393 Therefore, we have

$$\begin{aligned} &\Pr_{x_i \leftarrow X} [A(QoC[x_i]) = b_i] \\ &\leq \Pr_{x_i \leftarrow X} [A(QoC[x_i]) = b_i \mid E(x_i)] \cdot \Pr_{x_i \leftarrow X} [E(x_i)] + \Pr_{x_i \leftarrow X} [\bar{E}(x_i)] \\ &\leq \Pr_{x_i \leftarrow X} [A(QoC[x_i]) = b_i \mid E(x_i)] \cdot \Pr_{x_i \leftarrow X} [E(x_i)] + \beta \\ &\leq \left(\Pr_{x_i \leftarrow X} [A(C[x_i]) = b_i \mid E(x_i)] + \alpha \right) \cdot \Pr_{x_i \leftarrow X} [E(x_i)] + \beta \\ &\leq \Pr_{x_i \leftarrow X} [A(C[x_i]) = b_i] + \alpha + \beta \\ &= \text{SQMI}(A, C, X) + \alpha + \beta. \end{aligned}$$

394

□

395 Now we are ready to state a corollary of Theorems 5 and 2 for the full pipeline of Split-AI followed by
 396 Self-Distillation. The following Corollary directly follows from Theorems 5 and 2.

397 **Corollary 6.** Let C_{ST} be a learner that uses the Split-AI algorithm 1. Also, let Q_{SD} be a distiller that uses
 398 self-distillation algorithm. If Q_{SD} is (α, β) -stable for a dataset X and distribution $\mathcal{M}_{C_{ST}, X}$, then, for any
 399 adversary A we have

$$\text{SQMI}(A, Q_{SD} \circ C_{ST}, X) \leq 0.5 + \alpha + \beta.$$

400 **Remark 7** (How private is SELENA against multi-query attacks?). *The above theoretical analysis of SELENA*
 401 *is only valid for single-query direct attacks. But one might wonder if we can show a similar theory for privacy of*
 402 *SELENA against multi-query attacks. Unfortunately, we cannot prove a result as general as Corollary 6 for*
 403 *multi-query attacks. In fact, there exist some datasets that SELENA cannot obtain provable privacy for. For*
 404 *instance, imagine a dataset that contains two points $(x, 0)$ and $(x', 1)$ in the dataset such that x and x' are*
 405 *almost the same points, i.e. $x \approx x'$, yet they are labeled differently in the training set (x is labeled as 0 and x'*
 406 *as 1). In this scenario, we can observe that the adversary can obtain information about membership of x and*
 407 *x' , when querying both points. In particular, if only one of x and x' are selected as members, then we expect*
 408 *the result of query on x and x' to be the same and equal to the label of the one that is selected as a member.*
 409 *However, we argue that this lack of privacy for certain datasets will not manifest in the real world examples as*
 410 *such high correlation does not appear in real-world datasets. Our empirical analysis of SELENA is consistent*
 411 *with this claim. We defer the theoretical analysis of SELENA for multi-query attacks on datasets that satisfy*
 412 *certain assumptions to future work.*

413 D Experimental setup

414 Here we introduce the datasets, the model architectures, and the hyper-parameter settings in more detail.

415 D.1 Dataset

416 We use three benchmark datasets widely used in prior works on MIAs:

417 **CIFAR100 [12]:** This is a benchmark dataset used to evaluate image classification algorithms. CIFAR100 is
 418 composed of 32×32 color images in 100 classes, with 600 images per class. For each class label, 500 images
 419 are used as training samples, and remaining 100 images are used as test samples.

420 **Purchase100 [19]:** This dataset is based on Kaggle’s Acquire Valued Shopper Challenge, which contains
 421 shopping records of several thousand individuals. We obtained a preprocessed and simplified version provided
 422 by Shokri et al. [23]. This dataset is composed of 197,324 data samples with 600 binary features. Each feature
 423 corresponds to a product and represents whether the individual has purchased it or not. This dataset is clustered
 424 into 100 classes corresponding to purchase styles.

425 **Texas100 [27]:** This dataset is based on the Hospital Discharge Data public use files with information about
 426 inpatients stays in several health facilities released by the Texas Department of State Health Services from 2006
 427 to 2009. Each data record contains external causes of injury, the diagnosis, the procedures the patient underwent
 428 and some generic information. We obtain a preprocessed and simplified version of this dataset provided by
 429 Shokri et al. [23], which is composed of 67,330 data samples with 6,170 binary features. This dataset is used to
 430 classify 100 most frequent used procedures.

431 D.2 Target Models

432 For CIFAR100, we use ResNet-18 [8], which is a benchmark machine learning model widely used in computer
 433 vision tasks. We adopt the cross-entropy loss function and use Stochastic Gradient Descent (SGD) to learn the
 434 model parameters. We train the model for 200 epochs with batch size of 256, initializing learning rate 0.1 with
 435 weight decay 0.0005 and Nesterov momentum of 0.9 and divide the learning rate by 5 at epoch 60, 120, 160.⁵

436 For Purchase100 and Texas100, we follow previous work [16] to use a 4-layer fully connected neural network
 437 with layer sizes [1024, 512, 256, 100] and Tanh as the activation function. We use the cross-entropy loss function
 438 and Adam [11] optimizer to train the model on Purchase100 for 30 epochs and on Texas100 for 20 epochs with
 439 learning rate of 0.001. The batch size is 512 for Purchase100 and 128 for Texas100.

440 E Comparison with other defenses

441 E.1 Comparison with early stopping

442 During the training process, the model may learn too much information in the training samples thus the difference
 443 between its behavior on members and non-members becomes larger and larger, and the model becomes more

⁵<https://github.com/weiaicunzai/pytorch-cifar100>

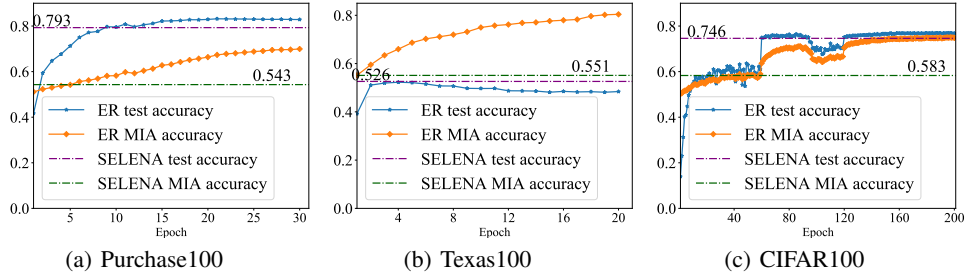


Figure 2: Detailed comparison of SELINA with early stopping. From left to right are results for Purchase100, Texas100 and CIFAR100. The solid curves are the test accuracy and MIA accuracy with corresponding training epochs. ER denotes early stopping. The dashed lines are the test accuracy and MIA accuracy of SELINA, which is shown in Table 1. Our defense achieves a better privacy-utility trade-off than all epochs in the conventional training.

444 vulnerable to membership inference attacks. Therefore, early stopping, which is a general technique to prevent
 445 model overfitting by stopping model training before the whole training process ends, can mitigate MIA accuracy
 446 with a sacrifice of model utility. Song et al. [25] find that adversarial regularization is not better than early
 447 stopping [4] when evaluated by a suite of attacks including both NN-based attacks and metric-based attacks.
 448 Therefore, we further compare our defense with early stopping.

449 Specifically, we will compare the model performance of an undefended model in each epoch during the training
 450 process and our final protected model $F_{\theta_{II}}$. For early stopping, we only consider direct single-query attack (due
 451 to their strong performance on undefended models). Figure 2 shows a detailed comparison between our defense
 452 $F_{\theta_{II}}$ and early stopping. The dashed lines are the classification accuracy on test set and the best MIA accuracy
 453 of our defense, which is already reported in Table 1. The solid lines correspond to classification accuracy on test
 454 set and MIA accuracy using the undefended model as a function of the training epochs. As we can see from
 455 Figure 2, *our defense significantly outperforms early stopping.*

456 **Comparison at similar attack accuracy.** The undefended model will only have same level of MIA accuracy
 457 as the dashed line of our defense at the very beginning of the training process. However the test accuracy of the
 458 undefended model at that point is far lower than that of our defense. For example, approximately, *for Texas100,*
 459 *when MIA accuracy against the conventional trained model is 55.1%, the test accuracy of the undefended model*
 460 *is 39.2%, which is 13.4% lower than that of our defense (52.6%).* For other two dataset, when the MIA accuracy
 461 against the undefended model achieves similar attack accuracy as our defense, the test accuracy is 8.0% lower
 462 on Purchase100 and 11.0% lower on CIFAR100 compared to our defense.

463 **Comparison at similar classification accuracy.** When the undefended model achieves the same classification
 464 accuracy on the test set as our defense, the MIA accuracy against the undefended model is significantly higher
 465 than our defense. For example, *when the test accuracy of the conventional model reaches 74.6% on CIFAR100*
 466 *(similar to our defense), the attack accuracy is 63.6%, compared to the best attack accuracy of 58.3% for*
 467 *our defense (which is 5.3% lower).* We can see similar results on other datasets: when the test accuracy of
 468 undefended models achieves similar classification accuracy as our defense on Purchase100 and Texas100, the
 469 attack accuracy is 58.1% on Purchase100 and 66.0% on Texas100, which is 3.8% and 10.9% higher than our
 470 defense separately.

471 E.2 Comparison with DP-SGD

472 We use the canonical implementation of DP-SGD and its associated analysis from the TensorFlow Privacy
 473 library⁶. We varied the parameter *noise_multiplier* in the range of [1, 3] on Purchase100 and [1, 2] on
 474 Texas100 with a step size 0.2. We set the privacy budget $\epsilon = 4$ and report the best classification accuracy for
 475 these two datasets.

476 The test accuracy on Purchase100 is 56.0% and the corresponding best direct single-query MIA accuracy is
 477 52.8%. The test accuracy on Texas100 is 39.1%, and the corresponding best direct single-query MIA accuracy is
 478 53.8%. Note that though DP-SGD provides a differential privacy guarantee and the best direct single-query MIA
 479 accuracy is 0.5% ~ 1% lower than that against our SELINA, DP-SGD suffers from a significant loss in utility:
 480 compared to the undefended model DP-SGD incurs 13.2% ~ 27.5% drop in classification accuracy, while our
 481 defense incurs no more than 3.9% drop in test accuracy.

⁶<https://github.com/tensorflow/privacy>